

LUMINA-SN

Monte Carlo Radiative Transfer for Type Ia Supernovae

A Complete Technical Manual

K. J. Han

February 2026

Copyright © 2026 K. J. Han

LUMINA-SN: LUMINOSITY-DRIVEN MONTE CARLO SUPERNOVA SPECTRAL SYNTHESIZER

This code implements 1D Monte Carlo radiative transfer in homologously expanding supernova ejecta, following the formalism of Lucy [3–5] and the TARDIS code [2]. Written in C99 with CUDA GPU acceleration.

Version 2.0 — February 2026

Contents

I Physics & Theory	7
1 Introduction to Type Ia Supernovae	9
1.1 What is a Type Ia Supernova?	9
1.2 The Expanding Ejecta	9
1.3 Spectral Features	9
1.4 The Inverse Problem	10
2 Radiative Transfer in Expanding Atmospheres	11
2.1 The Transfer Equation	11
2.2 The Sobolev Approximation	11
2.3 The Dilute Radiation Field	12
2.4 Frame Transformations	12
2.5 Bound–Free and Free–Free Opacity	12
3 Monte Carlo Photon Transport	13
3.1 The Indivisible Energy Packet Formalism	13
3.2 Packet Initialization	13
3.2.1 Frequency Sampling from the Planck Function	13
3.2.2 Angular Distribution	14
3.3 The Packet Propagation Loop	14
3.4 Distance Calculations	14
3.4.1 Distance to Shell Boundary	14
3.4.2 Distance to Electron Scattering	14
3.4.3 Distance to Sobolev Resonance	14
3.5 Line Interaction Types	15
3.5.1 Resonant Scattering (Mode 0)	15
3.5.2 Downbranching (Mode 1)	15
3.5.3 Macro-Atom (Mode 2)	15
3.6 Monte Carlo Estimators	15
3.7 Convergence: The Iteration Loop	16

II	Code Architecture	17
4	Overview & Build System	19
4.1	File Structure	19
4.2	Build System	19
4.3	Dependencies	20
4.4	Execution	20
5	Data Structures	21
5.1	The RPacket Structure	21
5.2	Geometry	21
5.3	Opacity State	22
5.4	Plasma State	22
5.5	Atomic Data	22
5.6	Monte Carlo Estimators	23
6	Transport Engine	25
6.1	Overview	25
6.2	The trace_packet Function	25
6.3	Sobolev Line Sweep	25
6.4	Thomson Scattering	26
6.5	Boundary Crossing	26
7	Plasma Physics Solver	27
7.1	Overview	27
7.2	Step 1: Partition Functions	27
7.3	Step 2: Electron Density	27
7.4	Step 3: Nebular Saha Ionization	28
7.5	Step 4: τ_{Sobolev} Update	28
7.6	Step 5: Radiation Field Update	28
8	Atomic Data System	29
8.1	Data Sources	29
8.2	The NPY Format Reader	29
8.3	The CSV Parser	29
9	CUDA GPU Implementation	31
9.1	Design Philosophy	31
9.2	Memory Layout	31
9.3	Kernel Launch Configuration	31
9.4	Random Number Generation	32
9.5	Atomic Estimator Updates	32

9.6	Performance	32
9.7	Resolved GPU Bugs	33
III	Usage & Applications	35
10	Installation & Quick Start	37
10.1	Prerequisites	37
10.2	Step-by-Step Setup	37
10.3	Input Directory Structure	38
10.4	Output Files	38
11	The Ejecta Model	39
11.1	Three-Zone Composition	39
11.2	Broken Power-Law Density	39
11.3	Physical Parameter Space	39
12	Parameter Fitting	41
12.1	Fitting Strategy	41
12.1.1	Phase 1: Coarse Exploration	41
12.1.2	Phase 2: Refinement	41
12.1.3	Phase 3: Production	41
12.2	Objective Function	41
13	Physical Constants & Reference Values	43
	Bibliography	45
	Index	47



Physics & Theory

1

Introduction to Type Ia Supernovae

1.1 What is a Type Ia Supernova?

A Type Ia supernova (SN Ia) is the thermonuclear explosion of a carbon-oxygen white dwarf star that has reached a critical mass near the Chandrasekhar limit ($M_{\text{Ch}} \approx 1.4 M_{\odot}$). The explosion completely unbinds the star, leaving no compact remnant, and synthesizes approximately $0.6 M_{\odot}$ of radioactive ^{56}Ni [7].

Important: SN Ia are cosmological standard candles: their peak luminosity correlates with their light-curve decline rate (the Phillips relation, [8]), enabling precise distance measurements to galaxies. This led to the discovery of the accelerating expansion of the Universe.

1.2 The Expanding Ejecta

After the explosion, the ejecta expand freely into a vacuum. Within hours, the expansion reaches a state of **homologous expansion**:

$$v(r, t) = \frac{r}{t} \quad (1.1)$$

where r is the radial distance from the center and t is the time since explosion. This means velocity maps directly to radius: faster material is farther out.

Definition 1.1 — Homologous Expansion. In homologous expansion, each fluid element moves at constant velocity. The density at any velocity coordinate v evolves as:

$$\rho(v, t) = \rho_0(v) \left(\frac{t_0}{t} \right)^3 \quad (1.2)$$

where $\rho_0(v)$ is the density at reference epoch t_0 , and the t^{-3} factor comes from the 3D volumetric dilution.

1.3 Spectral Features

SN Ia spectra are dominated by **P Cygni profiles**: blueshifted absorption troughs paired with redshifted emission peaks. These arise because:

1. Material approaching the observer (along the line of sight) absorbs photons at a blueshifted wavelength.
2. The surrounding envelope re-emits photons isotropically, producing a net emission component redward of the rest wavelength.

Table 1.1: Key spectral features in SN Ia near maximum light.

Ion	Rest λ (Å)	Observed Range (Å)	Diagnostic Value
Si II	6355	5800–6500	Expansion velocity, temperature
Si II	5972	5600–6000	Temperature indicator
S II	5454, 5640	5200–5700	“W” feature, burning completeness
Ca II	3934, 3968	3600–4000	H&K lines, high-velocity features
Ca II	8498, 8542, 8662	8000–8800	IR triplet
Fe II	4500–5200	4300–5200	Iron-group blanketing
O I	7774	7400–7900	Unburned oxygen indicator

1.4 The Inverse Problem

Given an observed spectrum, we want to determine the physical parameters of the explosion:

- Luminosity L and photospheric temperature T_{inner}
- Density profile $\rho(v)$ and its power-law exponents
- Chemical composition as a function of velocity (abundance tomography)
- Time since explosion t_{exp}

LUMINA-SN solves the *forward problem*: given these parameters, compute the emergent spectrum. Combined with Bayesian inference (Part III), this enables solving the inverse problem.



Radiative Transfer in Expanding Atmospheres

2.1 The Transfer Equation

The specific intensity I_ν along a ray satisfies:

$$\frac{dI_\nu}{ds} = -\kappa_\nu I_\nu + j_\nu \quad (2.1)$$

where s is the path length, κ_ν is the absorption coefficient (opacity), and j_ν is the emissivity.

In a supernova atmosphere, three opacity sources contribute:

1. **Electron scattering** (Thomson): frequency-independent, $\sigma_T = 6.652 \times 10^{-25} \text{ cm}^2$
2. **Line opacity** (Sobolev): resonant absorption in atomic transitions
3. **Continuum opacity**: bound-free and free-free (negligible in SN Ia, see §2.5)

2.2 The Sobolev Approximation

In homologous expansion, the velocity gradient $dv/dr = 1/t_{\exp}$ is constant. A photon sweeps through a line's resonance frequency over a very short distance (the *Sobolev length*). This means line interactions are *local*: each line either absorbs the photon or lets it pass.

Definition 2.1 — Sobolev Optical Depth. The optical depth of a line transition $l \rightarrow u$ in the Sobolev approximation is:

$$\tau_{\text{Sob}} = \frac{\pi e^2}{m_e c} f_{lu} \lambda_0 t_{\exp} n_l \left(1 - \frac{g_l n_u}{g_u n_l} \right) \quad (2.2)$$

where f_{lu} is the oscillator strength, λ_0 is the rest wavelength, n_l and n_u are the lower and upper level populations, and g_l , g_u are the statistical weights.

The numerical coefficient is:

$$\frac{\pi e^2}{m_e c} = 0.02654 \text{ cm}^2 \text{ s}^{-1} \quad (\text{CGS}) \quad (2.3)$$

The *escape probability* from a Sobolev line is:

$$\beta_{\text{Sob}} = \frac{1 - e^{-\tau_{\text{Sob}}}}{\tau_{\text{Sob}}} \quad (2.4)$$

2.3 The Dilute Radiation Field

Far from the photosphere, the radiation field is diluted. The mean intensity is:

$$J_\nu = W B_\nu(T_{\text{rad}}) \quad (2.5)$$

where W is the **dilution factor** and T_{rad} is the **radiation temperature**. For a geometrically thin photosphere at radius R_{phot} :

$$W(r) = \frac{1}{2} \left(1 - \sqrt{1 - \left(\frac{R_{\text{phot}}}{r} \right)^2} \right) \quad (2.6)$$

Remark 2.1 — Physical Interpretation of W . At $r = R_{\text{phot}}$: $W = 0.5$ (hemisphere illuminated). At $r \gg R_{\text{phot}}$: $W \approx R_{\text{phot}}^2/(4r^2) \rightarrow 0$ (point source). In practice, Monte Carlo estimators yield W values that include the effects of line scattering and fluorescence.

2.4 Frame Transformations

In homologous expansion, the comoving-frame (CMF) frequency differs from the lab-frame frequency:

$$\nu_{\text{cmf}} = \nu_{\text{lab}} \left(1 - \frac{\mu v}{c} \right) = \nu_{\text{lab}} \left(1 - \frac{\mu r}{c t_{\text{exp}}} \right) \quad (2.7)$$

where $\mu = \cos \theta$ is the direction cosine of the photon with respect to the radial direction, and $v = r/t_{\text{exp}}$.

Important: As a photon propagates through a shell, the comoving-frame frequency changes *linearly* with distance s along the ray:

$$\nu_{\text{cmf}}(s) = \nu_{\text{lab}} \left(1 - \frac{r_0 \mu_0 + s}{c t_{\text{exp}}} \right) \quad (2.8)$$

This monotonic frequency sweep is the basis of the Sobolev sweep algorithm (§3.4.3).

2.5 Bound–Free and Free–Free Opacity

In SN Ia ejecta, continuum opacities are negligible because:

- **Bound–free:** Optical photons (1.5–2.5 eV) are far below the ionization thresholds of the dominant species (Si II: 16.35 eV, Fe II: 16.19 eV, Ca II: 11.87 eV). Only far-UV photons ($< 1000 \text{ \AA}$) could ionize these ions.
- **Free–free:** Electron densities are very low ($n_e \sim 10^9 \text{ cm}^{-3}$ inner, $\sim 10^6 \text{ cm}^{-3}$ outer), giving $\kappa_{\text{ff}} \sim 10^{-20} \text{ cm}^{-1}$.

The combined continuum optical depth across a shell is $\tau_{\text{cont}} \sim 10^{-6}$ to 10^{-9} , confirming that **line opacity dominates** the spectrum formation in SN Ia.

3

Monte Carlo Photon Transport

3.1 The Indivisible Energy Packet Formalism

LUMINA follows the Lucy [3, 4] formalism, where photons are represented as discrete **energy packets** (*r*-packets) with properties:

Table 3.1: Properties of an *r*-packet in LUMINA.

Symbol	Description	Unit
r	Radial position	cm
μ	Direction cosine ($\cos \theta$)	–
ν	Lab-frame frequency	Hz
ε	Packet energy	erg
i_{shell}	Current shell index	–

All packets carry the same energy:

$$\varepsilon_{\text{pkt}} = \frac{L_{\text{inner}} \Delta t}{N_{\text{packets}}} \quad (3.1)$$

where L_{inner} is the luminosity at the inner boundary and Δt is the simulation time interval.

3.2 Packet Initialization

Packets are emitted from the photosphere ($r = R_{\text{inner}}$) with:

3.2.1 Frequency Sampling from the Planck Function

The emission frequency is sampled from a blackbody at temperature T_{inner} using the Bjorkman and Wood [1] method:

1. Draw $\xi_0 \sim U(0, 1)$
 2. Find l_{\min} such that $\sum_{i=1}^{l_{\min}} i^{-4} \geq \frac{\pi^4}{90} \xi_0$
 3. Draw $\xi_1, \xi_2, \xi_3, \xi_4 \sim U(0, 1)$
 4. Compute $x = -\ln(\xi_1 \xi_2 \xi_3 \xi_4)/l_{\min}$
 5. Set $\nu = x k_B T_{\text{inner}}/h$
- This is exact (no rejection) and samples directly from $B_{\nu}(T)$.

3.2.2 Angular Distribution

The direction cosine is sampled from a limb-darkened distribution:

$$\mu = \sqrt{\xi}, \quad \xi \sim U(0, 1) \quad (3.2)$$

ensuring that more packets are emitted along the normal direction.

3.3 The Packet Propagation Loop

Each packet undergoes a loop until it escapes ($r > R_{\text{outer}}$) or is reabsorbed ($r < R_{\text{inner}}$ moving inward):

Algorithm: Single Packet Loop

1. **Draw random optical depth:** $\tau_{\text{event}} = -\ln(\xi)$
2. **Compute distances** to possible events:
 - d_{boundary} : distance to next shell wall
 - d_{line} : distance to next Sobolev resonance
 - d_e : distance to electron scattering ($\tau = n_e \sigma_T d$)
3. **Select minimum:** $d_{\min} = \min(d_{\text{boundary}}, d_{\text{line}}, d_e)$
4. **Move packet:** update r, μ , accumulate estimators
5. **Handle interaction:**
 - Boundary: change shell, check escape/reabsorption
 - Line: scatter, downbranch, or activate macro-atom
 - Electron: Thomson scatter (isotropic re-emission)
6. **Repeat** from step 1

3.4 Distance Calculations

3.4.1 Distance to Shell Boundary

For a packet at (r, μ) in shell $[r_{\text{in}}, r_{\text{out}}]$:

Outward ($\mu > 0$ or $r > r_{\text{in}}/\mu$):

$$d_{\text{out}} = \sqrt{r_{\text{out}}^2 - r^2(1 - \mu^2)} - r\mu \quad (3.3)$$

Inward ($\mu < 0$ and impact parameter $< r_{\text{in}}$):

$$d_{\text{in}} = -r\mu - \sqrt{r_{\text{in}}^2 - r^2(1 - \mu^2)} \quad (3.4)$$

3.4.2 Distance to Electron Scattering

$$d_e = \frac{\tau_{\text{event}}}{n_e \sigma_T} \quad (3.5)$$

3.4.3 Distance to Sobolev Resonance

As the packet traverses the shell, the CMF frequency sweeps through the line list. For a line at rest frequency ν_{line} :

$$d_{\text{line}} = \frac{\nu_{\text{cmf}}(r, \mu) - \nu_{\text{line}}}{\nu_{\text{lab}}} c t_{\text{exp}} \quad (3.6)$$

Important: The Sobolev sweep must scan from the *entry* frequency to the *exit* frequency of each shell. The original LUMINA code used a fixed $\pm 1\%$ window, which missed lines during thick shell crossings. The corrected algorithm (Task #067) uses the full Doppler sweep, increasing line interactions from 0.6% to $> 50\%$ of packet steps.

3.5 Line Interaction Types

When a packet encounters a line, three interaction modes are available:

3.5.1 Resonant Scattering (Mode 0)

The packet is absorbed and re-emitted at the same line frequency with a new random direction:

$$\mu_{\text{new}} \sim U(-1, +1), \quad \nu_{\text{new}} = \nu_{\text{line}} \quad (3.7)$$

3.5.2 Downbranching (Mode 1)

The packet is absorbed into the upper level and re-emitted in a *different* line, selected from the downbranching probability distribution:

$$P(\text{emit in line } j) = \frac{A_{u \rightarrow l_j}}{\sum_k A_{u \rightarrow l_k}} \quad (3.8)$$

This enables fluorescence: a UV photon absorbed in one line can be re-emitted in the optical.

3.5.3 Macro-Atom (Mode 2)

The full macro-atom formalism [4, 5] activates the atom at the upper energy level and follows a Markov chain of internal transitions:

Algorithm: Macro-Atom Transition Walk

1. Start at activation level l
 2. Look up transition block for level l (list of possible transitions)
 3. Draw $\xi \sim U(0, 1)$, select transition k from cumulative probabilities
 4. If transition type ≥ 0 (internal): move to destination level, go to step 2
 5. If transition type < 0 (emission): emit in the associated line, **exit**
- Maximum 500 iterations (safety limit).

Emission types include:

- -1: Bound-bound emission (emit photon in a specific line)
- -2: Bound-free emission (photoionization, thermalization)
- -3: Free-free emission (thermal)
- -4: Adiabatic cooling

3.6 Monte Carlo Estimators

As packets propagate, they contribute to estimators that probe the radiation field.

Definition 3.1 — Mean Intensity Estimator.

$$\hat{J}_\nu = \frac{1}{4\pi V \Delta t} \sum_{\text{packets}} \varepsilon_{\text{cmf}} \Delta s \quad (3.9)$$

In practice, two scalar estimators are accumulated per shell:

$$j = \sum_{\text{packets}} \varepsilon_{\text{cmf}} \Delta s \quad (3.10)$$

$$\bar{\nu} = \frac{\sum_{\text{packets}} \varepsilon_{\text{cmf}} \nu_{\text{cmf}} \Delta s}{\sum_{\text{packets}} \varepsilon_{\text{cmf}} \Delta s} \quad (3.11)$$

From these, the radiation temperature and dilution factor are recovered:

$$T_{\text{rad}} = T_{\text{rad, const}} \times \frac{\bar{\nu}}{j} \quad (3.12)$$

$$W = \frac{j}{4 \sigma_{\text{SB}} T_{\text{rad}}^4 \Delta t V} \quad (3.13)$$

where $T_{\text{rad, const}} = \frac{\pi^4}{15 \cdot 24 \cdot \zeta(5)} \frac{h}{k_B} = 1.2523 \times 10^{-11}$ K·s.

3.7 Convergence: The Iteration Loop

LUMINA iterates between transport and plasma calculations:

1. **Transport:** Run N_{packets} through the ejecta, accumulating estimators.
2. **Radiation field update:** Compute T_{rad}, W from estimators, with **damping**:

$$X_{\text{new}} = X_{\text{old}} + d \cdot (X_{\text{est}} - X_{\text{old}}), \quad d = 0.5 \quad (3.14)$$

3. **Plasma update:** Recompute ionization, level populations, τ_{Sob} .

4. **T_{inner} update** (after hold iterations):

$$T_{\text{inner,new}} = T_{\text{inner,old}} + d \cdot \left[T_{\text{inner}} \left(\frac{L_{\text{emitted}}}{L_{\text{requested}}} \right)^{-0.5} - T_{\text{inner,old}} \right] \quad (3.15)$$

Remark 3.1 — Exponent -0.5 vs $+0.25$. Naïvely, Stefan–Boltzmann gives $T \propto L^{0.25}$, suggesting the correction factor should be $(L_{\text{em}}/L_{\text{req}})^{0.25}$. However, TARDIS uses the exponent -0.5 because changing T_{inner} also changes the opacity (through ionization), leading to non-linear feedback. The empirical -0.5 accounts for this.



Code Architecture

4

Overview & Build System

4.1 File Structure

LUMINA-SN consists of the following source files:

Table 4.1: Source files and their roles.

File	Lines	Purpose
lumina.h	378	Master header: all structures, constants, prototypes
lumina_transport.c	515	CPU transport kernel
lumina_plasma.c	524	Plasma solver & convergence
lumina_atomic.c	700	Atomic data loading (HDF5, CSV, NPY)
lumina_main.c	466	Main driver & iteration loop
lumina_cuda.cu	1353	CUDA GPU transport kernel
Total	3936	

4.2 Build System

Listing 4.1: Building LUMINA-SN

```
1 # CPU build (serial)
2 make
3
4 # CPU build with OpenMP parallelism
5 make OMP=1
6
7 # CUDA GPU build
8 make cuda
```

Important: `make clean` deletes CSV output files. Always save important spectral outputs before rebuilding.

Table 4.2: Compiler flags.

Target	Compiler	Flags
CPU	gcc	-O2 -Wall -Wextra -std=c11 -lm
CPU+OMP	gcc	adds -fopenmp
GPU	nvcc	-O2 -arch=sm_89 -std=c++14

4.3 Dependencies

- **HDF5** (optional): For loading atomic data from `kurucz_cd23_chianti_H_He.h5`
- **CUDA Toolkit ≥ 12.0** : For GPU builds (tested with CUDA 13.0, sm_89)
- **OpenMP**: For CPU parallelism (optional)
- **Standard C library**: `math.h`, `stdio.h`, `stdlib.h`, `string.h`

4.4 Execution

Listing 4.2: Running LUMINA-SN

```

1 # CPU: reference model with 200K packets, 20 iterations
2 ./lumina_tardis_reference 200000 20
3
4 # CUDA: same with GPU acceleration
5 ./lumina_cuda_atomic/kurucz_cd23_chianti_H_He.h5 200000 output.csv

```

5 Data Structures

5.1 The RPacket Structure

The fundamental unit of the Monte Carlo simulation:

Listing 5.1: RPacket — photon energy packet

```
1  typedef struct {
2      double r;                      // radial position [cm]
3      double mu;                    // cos(theta) direction
4      double nu;                    // lab-frame frequency [Hz]
5      double energy;                // packet energy [erg]
6      int current_shell_id;        // shell index [0..n_shells-1]
7      int next_line_id;            // Sobolev sweep bookmark
8      PacketStatus status;        // IN_PROCESS / EMITTED /
9          REABSORBED
10     int index;                  // packet ID (for RNG seeding)
11 } RPacket;
```

5.2 Geometry

The 1D spherically symmetric ejecta model:

Listing 5.2: Geometry — shell structure

```
1  typedef struct {
2      int n_shells;                // number of shells (default: 30)
3      double *r_inner;             // [n_shells] inner radii [cm]
4      double *r_outer;             // [n_shells] outer radii [cm]
5      double *v_inner;              // [n_shells] inner velocities [cm/
6          s]
7      double *v_outer;              // [n_shells] outer velocities [cm/
8          s]
9      double time_explosion;       // t_exp [seconds]
10 } Geometry;
```

The radii are derived from velocities via homologous expansion: $r = v \times t_{\text{exp}}$.

5.3 Opacity State

Pre-computed opacity data used during transport:

Listing 5.3: `OpacityState` — line and continuum opacities

```

1  typedef struct {
2      int n_lines, n_shells;
3      double *line_list_nu;           // [n_lines] rest frequencies,
4                                     // descending
5      double *tau_sobolev;          // [n_lines * n_shells]
6      double *electron_density;     // [n_shells] n_e [cm^-3]
7      double *t_electrons;         // [n_shells] T_e [K]
8
9      // Macro-atom transition data
10     int n_macro_levels, n_macro_transitions;
11     int *macro_block_references;    // [n_levels+1]
12     int *transition_type;         // [n_transitions]
13     int *destination_level_id;    // [n_transitions]
14     int *transition_line_id;      // [n_transitions]
15     double *transition_probabilities; // [n_transitions *
16                                     // n_shells]
16     int *line2macro_level_upper;   // [n_lines]
16 } OpacityState;
```

Remark 5.1 — Line List Ordering. Lines are sorted in *descending* frequency order. As a packet's CMF frequency decreases while traversing a shell, it encounters lines from high to low frequency. This ordering enables efficient forward-only scanning.

5.4 Plasma State

Thermodynamic state updated each iteration:

Listing 5.4: `PlasmaState` — radiation field quantities

```

1  typedef struct {
2      int n_shells;
3      double *W;                  // [n_shells] dilution factor
4      double *T_rad;             // [n_shells] radiation temperature
5                                     // [K]
6      double *rho;               // [n_shells] mass density [g/cm^3]
7      double *n_electron;        // [n_shells] electron density [cm
8                                     ^-3]
8      double T_e_T_rad_ratio;   // default: 0.9
8 } PlasmaState;
```

5.5 Atomic Data

Comprehensive atomic physics database for the plasma solver:

Listing 5.5: `AtomicData` — atomic physics for Saha–Boltzmann

```

1  typedef struct {
2      // Per-line data
3      int *line_atomic_number;      // [n_lines] Z
4      int *line_ion_number;        // [n_lines] ionization stage
5      double *line_f_lu;          // [n_lines] oscillator
6          strength
7      double *line_wavelength_cm; // [n_lines] rest wavelength
8
9      // Energy levels
10     int n_levels;
11     double *level_energy_eV;    // [n_levels]
12     int *level_g;             // [n_levels] statistical
13         weight
14     int *level_metastable;    // [n_levels] 0 or 1
15
16      // Ionization energies
17     int n_ionization;
18     double *ioniz_energy_eV;   // [n_ionization]
19
20      // Zeta correction factors (dilute non-LTE)
21     double *zeta_data;        // [n_zeta_ions *
22         n_zeta_temps]
23
24      // Abundances
25     double *abundances;       // [n_elements * n_shells]
26
27 } AtomicData;

```

5.6 Monte Carlo Estimators

Accumulated during transport, used to update the radiation field:

Listing 5.6: `Estimators` — radiation field accumulators

```

1  typedef struct {
2      double *j_estimator;        // [n_shells] integral of E*ds
3      double *nu_bar_estimator;  // [n_shells] integral of E*nu*
4          ds
5      double *j_blue_estimator;   // [n_lines * n_shells] (CPU
6          only)
7      double *Edotlu_estimator;  // [n_lines * n_shells] (CPU
8          only)
9  } Estimators;

```

Remark 5.2 — GPU Limitation. The `j_blue` and `Edotlu` estimators are *not computed* on the GPU because they require $n_{\text{lines}} \times n_{\text{shells}} \approx 4$ million atomic additions per iteration — prohibitively expensive for `atomicAdd`.

6 Transport Engine

6.1 Overview

The transport engine (`lumina_transport.c`, 515 lines) propagates r -packets through the ejecta. It is the most performance-critical component.

6.2 The `trace_packet` Function

This function computes the next interaction event for a packet:

1. Compute distance to shell boundaries (d_{boundary})
2. Scan the Sobolev line list for resonances (d_{line} , accumulated τ)
3. Compute distance to electron scattering ($d_e = \tau_{\text{event}} / (n_e \sigma_T)$)
4. Return the minimum distance and interaction type

6.3 Sobolev Line Sweep

The sweep algorithm processes lines in descending frequency order:

Listing 6.1: Sobolev sweep (simplified)

```
1  double tau_trace_combined = 0.0;
2  for (int j = pkt->next_line_id; j < n_lines; j++) {
3      double nu_line = line_list_nu[j];
4      double d_line = compute_d_line(pkt, nu_line);
5
6      if (d_line < 0 || d_line > d_boundary) break;
7
8      double tau_line = tau_sobolev[j * n_shells + shell_id];
9      tau_trace_combined += tau_line;
10
11     if (tau_trace_combined > tau_event) {
12         // Line interaction!
13         *interaction_type = INTERACTION_LINE;
14         *d_min = d_line;
15         pkt->next_line_id = j;
16         return;
17     }
18 }
```

6.4 Thomson Scattering

Elastic scattering with free electrons:

1. Transform packet energy/frequency to comoving frame at current angle
2. Sample new direction: $\mu_{\text{new}} \sim U(-1, +1)$ (isotropic in CMF)
3. Transform back to lab frame with new angle
4. Energy is conserved in the comoving frame

$$\varepsilon_{\text{lab,new}} = \varepsilon_{\text{cmf}} \times \frac{1}{1 - \mu_{\text{new}} \cdot v/c} \quad (6.1)$$

6.5 Boundary Crossing

When a packet crosses a shell boundary:

1. Update shell index: $i_{\text{shell}} \leftarrow i_{\text{shell}} + \delta$ where $\delta = +1$ (outward) or -1 (inward)
2. Nudge position by $\epsilon = 10^{-10} \times \Delta r_{\text{shell}}$ into the new shell
3. Check for escape ($i > n_{\text{shells}} - 1$) or reabsorption ($i < 0$, inward-moving)

Important: The position nudge is critical. Without it, the packet lands exactly on the boundary, and the next distance calculation returns $d = 0$, causing an infinite loop (Task #024).

7

Plasma Physics Solver

7.1 Overview

The plasma solver (`lumina_plasma.c`, 524 lines) computes the thermodynamic state of the ejecta for each iteration. It implements the TARDIS-compatible nebular approximation [6].

7.2 Step 1: Partition Functions

The partition function for ion (Z , stage) in shell s is:

$$\mathcal{Z}(Z, \text{stage}, s) = \underbrace{\sum_{i \in \text{meta}} g_i e^{-E_i/k_B T_{\text{rad}}(s)}}_{\mathcal{Z}_{\text{meta}}} + W(s) \cdot \underbrace{\sum_{i \in \text{non-meta}} g_i e^{-E_i/k_B T_{\text{rad}}(s)}}_{\mathcal{Z}_{\text{non}}} \quad (7.1)$$

Important: The Boltzmann factors use T_{rad} for *all* levels (both metastable and non-metastable). Earlier code incorrectly used T_e for metastable levels. The dilution factor W suppresses the non-metastable contribution at large distances from the photosphere.

7.3 Step 2: Electron Density

Computed iteratively with TARDIS-style damping:

Algorithm: Electron Density Iteration

1. Start with initial guess $n_e^{(0)}$
2. For each element: compute ionization ratios using nebular Saha (Eq. 7.2)
3. Normalize ion populations to element abundance
4. Compute $n_e^{(\text{calc})} = \sum_{\text{ions}} \text{stage} \times n_{\text{ion}}$
5. Damped update: $n_e^{(k+1)} = 0.5 \times n_e^{(\text{calc})} + 0.5 \times n_e^{(k)}$
6. Convergence: $|n_e^{(k+1)} - n_e^{(k)}|/n_e^{(k)} < 0.05$

7.4 Step 3: Nebular Saha Ionization

The ionization ratio between consecutive stages is:

$$\boxed{\frac{n_{i+1}}{n_i} = \frac{\Phi_{\text{neb}}}{n_e}} \quad (7.2)$$

where the nebular ionization coefficient Φ_{neb} is:

$$\Phi_{\text{neb}} = \Phi_{\text{LTE}} \times W \times [\zeta \cdot \delta + W \cdot (1 - \zeta)] \times \sqrt{\frac{T_e}{T_{\text{rad}}}} \quad (7.3)$$

$$\Phi_{\text{LTE}} = \frac{\mathcal{Z}_{i+1}}{\mathcal{Z}_i} \times 2 \times g_e \times e^{-\chi/k_B T_{\text{rad}}} \quad (7.4)$$

$$g_e = \left(\frac{2\pi m_e k_B T_{\text{rad}}}{h^2} \right)^{3/2} \quad (7.5)$$

$$\delta = \frac{T_e}{T_{\text{rad}}} \exp \left[\chi \left(\frac{1}{k_B T_{\text{rad}}} - \frac{1}{k_B T_e} \right) \right] \quad (7.6)$$

Here χ is the ionization energy, and ζ is a non-LTE correction factor interpolated from tabulated values.

7.5 Step 4: τ_{Sobolev} Update

With ion populations known, τ_{Sob} is recomputed for each line and shell using Eq. (2.2). The level populations follow the Boltzmann distribution within each ion:

$$n_{l,\text{meta}} = \frac{g_l}{\mathcal{Z}} n_{\text{ion}} e^{-E_l/k_B T_{\text{rad}}}, \quad n_{l,\text{non}} = W \times \frac{g_l}{\mathcal{Z}} n_{\text{ion}} e^{-E_l/k_B T_{\text{rad}}} \quad (7.7)$$

7.6 Step 5: Radiation Field Update

From the MC estimators j and $\bar{\nu}$ (Eqs. 3.10–3.11):

$$T_{\text{rad,est}}(s) = 1.2523 \times 10^{-11} \times \frac{\bar{\nu}(s)}{j(s)} \quad [\text{K}] \quad (7.8)$$

$$W_{\text{est}}(s) = \frac{j(s)}{4 \sigma_{\text{SB}} T_{\text{rad}}^4(s) \Delta t V(s)} \quad (7.9)$$

All quantities are damped:

$$X_{\text{new}} = X_{\text{old}} + 0.5 \times (X_{\text{est}} - X_{\text{old}}) \quad (7.10)$$

8

Atomic Data System

8.1 Data Sources

LUMINA uses the TARDIS reference atomic dataset, originally from Kurucz CD23 and CHIANTI:

Table 8.1: Atomic data files.

File	Format	Contents
line_list.csv	CSV	ν , Z , ion, f_{lu} , λ per line
levels.csv	CSV	E (eV), g , metastable flag per level
ionization_energies.csv	CSV	χ per ion
tau_sobolev.npy	NPY	τ_{Sob} reference values
transition_probabilities.npy	NPY	Macro-atom transition probs
macro_atom_data.csv	CSV	Transition types, destinations
zeta_data.npy	NPY	Non-LTE correction factors
abundances.csv	CSV	Mass fractions per shell

8.2 The NPY Format Reader

LUMINA includes a custom NPY reader (no NumPy dependency in C):

1. Read 6-byte magic: \x93NUMPY
2. Read version (1 or 2) and header length
3. Parse Python dict header for `shape`, `dtype`, `fortran_order`
4. Read raw binary data
5. Transpose if Fortran-ordered

8.3 The CSV Parser

Important: The `macro_atom_data.csv` header starts with an unnamed index column: “,atomic_number,...”. The standard `strtok()` function skips leading delims.

iters, causing a column offset of -1 . LUMINA uses a manual field-by-field parser that handles empty fields correctly.

9

CUDA GPU Implementation

9.1 Design Philosophy

The GPU implementation maps **one CUDA thread per packet**. Each thread independently propagates its packet through the ejecta, requiring no inter-thread communication except for atomic estimator updates.

9.2 Memory Layout

Table 9.1: GPU memory allocation.

Data	Access	Size (200K pkts)
Line frequencies	Read-only	$n_{\text{lines}} \times 8 \text{ B}$
τ_{Sob}	Read-only	$n_{\text{lines}} \times n_{\text{shells}} \times 8 \text{ B}$
Transition probs	Read-only	$n_{\text{trans}} \times n_{\text{shells}} \times 8 \text{ B}$
Shell geometry	Read-only	$n_{\text{shells}} \times 4 \times 8 \text{ B}$
RNG states	Read/write	$N_{\text{pkt}} \times 4 \times 8 \text{ B}$
$j, \bar{\nu}$ estimators	Atomic write	$n_{\text{shells}} \times 2 \times 8 \text{ B}$
Output arrays	Write-only	$N_{\text{pkt}} \times 3 \times 8 \text{ B}$

Total GPU memory: approximately 2 GB for a typical run.

9.3 Kernel Launch Configuration

Listing 9.1: Kernel launch

```
1 int threads_per_block = 256;
2 int blocks = (n_packets + threads_per_block - 1)
3           / threads_per_block;
4 // Max blocks: 131072 (was 1024 -- critical bug #13)
5 transport_kernel<<<blocks, threads_per_block>>>(...);
```

Important: The original code had `CUDA_MAX_BLOCKS = 1024`, limiting execution to 262K packets regardless of N_{packets} . For 2M packets, only 13% executed, causing $j_{\text{estimator}}$ to be 76 \times too low. This was the single largest GPU bug (Task #13).

9.4 Random Number Generation

Each thread uses an independent `xoshiro256**` generator with 256 bits of state ($4 \times \text{uint64}$). Seeds are derived from the packet index via SplitMix64:

Listing 9.2: Per-thread RNG initialization

```

1  __device__ void init_rng(uint64_t *state, uint64_t seed) {
2      // SplitMix64 to expand seed into 4 state words
3      state[0] = splitmix64(&seed);
4      state[1] = splitmix64(&seed);
5      state[2] = splitmix64(&seed);
6      state[3] = splitmix64(&seed);
7  }
```

9.5 Atomic Estimator Updates

The j and $\bar{\nu}$ estimators are updated using CUDA `atomicAdd`:

Listing 9.3: Estimator accumulation on GPU

```

1  __device__ void update_estimators(
2      double *d_j_est, double *d_nu_bar_est,
3      int shell_id, double comov_energy,
4      double comov_nu, double distance)
5  {
6      atomicAdd(&d_j_est[shell_id],
7                 comov_energy * distance);
8      atomicAdd(&d_nu_bar_est[shell_id],
9                 comov_energy * distance * comov_nu);
10 }
```

Since there are only $n_{\text{shells}} = 30$ accumulation targets, contention is manageable.

9.6 Performance

Table 9.2: CPU vs GPU performance (NVIDIA RTX 5000 Ada, sm_89).

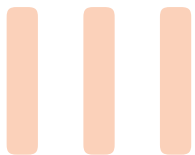
N_{packets}	CPU (1 core)	CPU (OMP64)	GPU	Speedup
20,000	0.7 s	0.1 s	0.08 s	9 \times
200,000	7.2 s	1.1 s	0.73 s	10 \times
2,000,000	72 s	11 s	7.3 s	10 \times
20,000,000	720 s	110 s	73 s	10 \times

Remark 9.1 — Statistical Accuracy. GPU and CPU produce statistically identical results. At 200K packets: W error 1.06%, T_{rad} error 0.58% (relative to TARDIS reference). The scaling follows $\sigma \propto N^{-0.35}$ to $N^{-0.40}$, close to Poisson ($N^{-0.5}$).

9.7 Resolved GPU Bugs

Four critical bugs were identified and fixed during development:

1. **MAX_BLOCKS = 1024**: Only 262K threads could launch. Fixed to 131072.
2. **Shared memory race**: `__shared__ ShellCache` shared by all 256 threads, but only thread 0 loaded data. Fixed: use L1-cached global memory.
3. **Counter accumulation**: Escape/reabsorb counters not reset between iterations. Fixed: explicit reset in `cuda_reset_estimators()`.
4. **Boundary sticking**: Packets land exactly on shell boundaries due to floating-point precision. Fixed: explicit nudge by $10^{-10} \times \Delta r$.



Usage & Applications

10

Installation & Quick Start

10.1 Prerequisites

Table 10.1: System requirements.

Component	Requirement
C Compiler	GCC \geq 9.0 (C11 support)
CUDA (optional)	Toolkit \geq 12.0, compute capability \geq 7.0
HDF5 (optional)	<code>libhdf5-dev</code> for atomic data loading
Memory	\geq 4 GB RAM (CPU), \geq 4 GB VRAM (GPU)

10.2 Step-by-Step Setup

Listing 10.1: Complete setup procedure

```
1 # Clone the repository
2 git clone git@github.com:kjhan0606/lumina-sn.git
3 cd lumina-sn
4
5 # Build CPU version
6 make
7
8 # (Optional) Build GPU version
9 make cuda
10
11 # Verify with a quick test (1000 packets, 5 iterations)
12 ./lumina tardis_reference 1000 5
13
14 # Production run (200K packets, 20 iterations)
15 ./lumina tardis_reference 200000 20
16
17 # Check output
18 head lumina_spectrum.csv
```

10.3 Input Directory Structure

LUMINA expects a reference data directory (default: `data/tardis_reference/`) containing:

Listing 10.2: Required input files

```

1  data/tardis_reference/
2    config.json                      # Simulation parameters
3    geometry.csv                     # Shell radii and velocities
4    density.csv                      # Mass density per shell
5    abundances.csv                  # Element mass fractions
6    electron_densities.csv          # Initial electron densities
7    plasma_state.csv                # Initial W, T_rad per shell
8    line_list.csv                   # Atomic line data
9    tau_sobolev.npy                 # Reference optical depths
10   transition_probabilities.npy
11   macro_atom_data.csv
12   macro_atom_references.csv
13   line2macro_level_upper.npy
14   levels.csv                      # Energy levels
15   ionization_energies.csv
16   zeta_ions.csv
17   zeta_temps.csv
18   zeta_data.npy
19   atom_masses.csv

```

10.4 Output Files

Table 10.2: Output files produced by LUMINA.

File	Contents
<code>lumina_spectrum.csv</code>	λ (Å) vs L_λ (erg/s/cm)
<code>lumina_plasma_state.csv</code>	Final W, T_{rad} per shell
<code>lumina_tau_validation.csv</code>	τ_{Sob} at shell 0 (debug)

11

The Ejecta Model

11.1 Three-Zone Composition

LUMINA uses a three-zone abundance structure motivated by SN Ia nucleosynthesis:

Table 11.1: Default three-zone composition model.

Zone	Fe	Si	S	Ca	Co	Ni	C	O
Core ($v < v_{\text{core}}$)	free	0.05	0.05	0.03	0.05	free	0.02	filler
Wall ($v_{\text{core}} - v_{\text{wall}}$)	free	free	0.05	0.03	0.05	free	0.02	filler
Outer ($v > v_{\text{wall}}$)	free	0.02	0.02	0.01	0.05	free	0.02	filler

“Filler” means oxygen fills the remaining mass fraction to ensure $\sum X_i = 1$.

Important: Oxygen is the correct filler element for the outer zone because it has very few optical absorption lines and is essentially transparent. Using Fe/Ni/S as fillers creates massive line blanketing ($> 10^6$ active lines) that produces an artificial pseudo-photosphere (Task #063).

11.2 Broken Power-Law Density

The density profile is a broken power law:

$$\rho(v) = \begin{cases} \rho_0 \left(\frac{v}{v_{\text{inner}}} \right)^{n_{\text{inner}}} & v < v_{\text{break}} \\ \rho_{\text{break}} \left(\frac{v}{v_{\text{break}}} \right)^{n_{\text{outer}}} & v \geq v_{\text{break}} \end{cases} \quad (11.1)$$

where $\rho_{\text{break}} = \rho_0 (v_{\text{break}}/v_{\text{inner}})^{n_{\text{inner}}}$ ensures continuity at v_{break} .

Typical values: $n_{\text{inner}} \approx -7$, $n_{\text{outer}} \approx -10$.

11.3 Physical Parameter Space

LUMINA-ML (the machine learning emulator companion) uses a 15-dimensional parameter space:

Table 11.2: Full 15D parameter space with ranges.

#	Parameter	Min	Max	Description
1	$\log L$	42.50	43.50	Luminosity [erg/s]
2	v_{inner}	7000	15000	Photosphere velocity [km/s]
3	$\log \rho_0$	-14.0	-12.3	Reference density [g/cm^3]
4	n_{inner}	-10	-4	Inner density exponent
5	T_e/T_{rad}	0.7	1.0	Temperature ratio
6	v_{core}	9000	17000	Core/wall boundary [km/s]
7	v_{wall}	12000	24000	Wall/outer boundary [km/s]
8	$X_{\text{Fe},\text{core}}$	0.05	0.85	Core iron abundance
9	$X_{\text{Si},\text{wall}}$	0.05	0.75	Wall silicon abundance
10	v_{break}	10000	22000	Density break velocity [km/s]
11	n_{outer}	-14	-4	Outer density exponent
12	t_{exp}	10	28	Time since explosion [days]
13	$X_{\text{Fe},\text{wall}}$	0.001	0.50	Wall iron contamination
14	X_{Ni}	0.005	0.25	Nickel abundance (all zones)
15	$X_{\text{Fe},\text{outer}}$	0.001	0.15	Outer iron abundance

12

Parameter Fitting

12.1 Fitting Strategy

LUMINA includes a multi-phase parameter search framework (`scripts/fit_parameter_search.py`) that combines Latin Hypercube Sampling with progressive refinement.

12.1.1 Phase 1: Coarse Exploration

- 200 Latin Hypercube samples across full parameter space
- 20K packets \times 5 iterations (fast, \sim 5 s per model)
- Score by feature-weighted RMS
- Select top-20 candidates

12.1.2 Phase 2: Refinement

- Top-20 candidates re-simulated with 100K packets \times 10 iterations
- Better statistics reduce Monte Carlo noise
- Select top-3

12.1.3 Phase 3: Production

- Top-3 candidates with 500K packets \times 20 iterations
- Highest-fidelity spectra
- Final selection based on composite score

12.2 Objective Function

The composite scoring function includes:

$$\text{Score} = \text{RMS}_{\text{spec}} + 0.5 |\Delta d_{\text{Si II}}| + 0.2 |\Delta \log v_{\text{Si II}}| + 0.1 |\Delta \lambda_{\min}| \quad (12.1)$$

where:

- RMS_{spec} : Spectral RMS over 5000–8000 Å
- $\Delta d_{\text{Si II}}$: Si II 6355 absorption depth error
- $\Delta \log v_{\text{Si II}}$: Si II velocity error (log scale)
- $\Delta \lambda_{\min}$: Si II trough wavelength error

13

Physical Constants & Reference Values

Table 13.1: Physical constants used in LUMINA (CGS).

Symbol	Description	Value
c	Speed of light	$2.99792458 \times 10^{10}$ cm/s
h	Planck constant	$6.62607015 \times 10^{-27}$ erg·s
k_B	Boltzmann constant	1.380649×10^{-16} erg/K
σ_{SB}	Stefan–Boltzmann	5.670374×10^{-5} erg/cm ² /s/K ⁴
σ_T	Thomson cross-section	6.6525×10^{-25} cm ²
m_e	Electron mass	9.10938×10^{-28} g
e	Electron charge	4.80321×10^{-10} esu
$\pi e^2/(m_e c)$	Sobolev coefficient	2.6540×10^{-2} cm ² /s
$T_{\text{rad,const}}$	T_{rad} estimator constant	1.2523×10^{-11} K·s

Bibliography

- [1] J. E. Bjorkman and K. Wood. “Radiative Equilibrium and Temperature Correction in Monte Carlo Radiation Transfer”. In: *The Astrophysical Journal* 554 (2001), pp. 615–623.
- [2] W. E. Kerzendorf and S. A. Sim. “A spectral synthesis code for rapid modelling of supernovae”. In: *Monthly Notices of the Royal Astronomical Society* 440 (2014), pp. 387–404. DOI: [10.1093/mnras/stu055](https://doi.org/10.1093/mnras/stu055).
- [3] L. B. Lucy. “Improved Monte Carlo techniques for the spectral synthesis of supernovae”. In: *Astronomy & Astrophysics* 345 (1999), pp. 211–220.
- [4] L. B. Lucy. “Monte Carlo techniques for time-dependent radiative transfer in 3-D supernovae”. In: *Astronomy & Astrophysics* 384 (2002), pp. 725–735.
- [5] L. B. Lucy. “Monte Carlo transition probabilities”. In: *Astronomy & Astrophysics* 403 (2003), pp. 261–275.
- [6] P. A. Mazzali and L. B. Lucy. “The application of Monte Carlo methods to the synthesis of early-time supernovae spectra”. In: *Astronomy & Astrophysics* 279 (1993), pp. 447–456.
- [7] K. Nomoto, F.-K. Thielemann, and K. Yokoi. “Accreting white dwarf models of Type I supernovae. III. Carbon deflagration supernovae”. In: *The Astrophysical Journal* 286 (1984), pp. 644–658.
- [8] M. M. Phillips. “The absolute magnitudes of Type IA supernovae”. In: *The Astrophysical Journal Letters* 413 (1993), pp. L105–L108.

Index

- Atomic Data, 29
 - CSV Parser, 29
 - NPY Format, 29
- Build System, 19
 - Makefile, 19
- Continuum Opacity, 12
- Convergence, 16
- CUDA, 31
 - Atomic Operations, 32
 - Bug Fixes, 33
 - Kernel Launch, 31
 - Memory Layout, 31
 - Performance, 32
 - RNG, 32
- Data Structures, 21
 - AtomicData, 22
 - Estimators, 23
 - Geometry, 21
 - OpacityState, 22
 - PlasmaState, 22
 - RPacket, 21
- Dilution Factor, 12
- Distance Calculations, 14
- Doppler
 - Frame Transformations, 12
- Ejecta
 - Homologous Expansion, 9
- Ejecta Model, 39
 - Density Profile, 39
 - Parameter Space, 39
 - Three-Zone, 39
- Energy Packets, 13
- Estimators, 15
 - Mean Intensity, 16
- Execution, 20
- Input Files, 38
- Installation, 37
- Line Interactions, 15
 - Downbranching, 15
 - Macro-Atom, 15
 - Resonant Scattering, 15
- Macro-Atom, 15
- Monte Carlo Methods, 13
- Output Files, 38
- Packet Initialization, 13
- Parameter Fitting, 41
 - Objective Function, 41
- Physical Constants, 43
- Plasma Solver, 27
 - Electron Density, 27
 - Partition Functions, 27
 - Radiation Field, 28
 - Saha Equation, 28
 - Tau Sobolev, 28
- Propagation Loop, 14
- Radiative Transfer, 11
 - Sobolev Approximation, 11
 - Sobolev Optical Depth, 11
 - Sobolev Sweep, 14
 - Spectral Features, 10
- Transfer Equation, 11
- Transport Engine, 25
 - Boundary Crossing, 26
 - Sobolev Sweep, 25
 - Thomson Scattering, 26
 - trace_packet, 25
- Type Ia Supernovae, 9